JOURNAL OF CATALYSIS 65, 207–220 (1980)

# Chemisorption Properties of Iridium on Alumina Catalysts

G. B. McVicker, R. T. K. Baker, R. L. Garten, and E. L. Kugler

*Exxon Research and Engineering Company, Corporate Research–Science Laboratories, Linden, New Jersey 07036*

Received January 29, 1980; revised April 14, 1980

Highly dispersed 0.3 to 1.0% iridium on alumina catalysts exhibit H/Ir and CO/Ir ratios near two for the strongly bound fraction of these adsorbates. Iridium particles in such catalysts are not detectable by high-resolution TEM which places an upper limit of 0.6 nm on their size. Increasing the metal concentration or oxidative calcination resulted in an increase in the average iridium particle size and a corresponding decrease in adsorbate/metal ratios. Average crystallite sizes calculated from chemisorption data and observed directly by TEM for partially agglomerated catalysts were found to be in good agreement. Infrared spectra of adsorbed carbon monoxide were observed to be dependent upon both iridium crystallite size and surface coverage. Under saturation coverage conditions (CO/Ir $> 1$), highly dispersed catalysts displayed a major carbonyl band at 2060 $cm^{-1}$. Agglomerated catalysts (CO/Ir $< 1$), in contrast, exhibit a band maxima centered in the 2020–2025 $cm^{-1}$ region. Taken together the chemisorption, TEM, and infrared data indicate that isolated iridium atoms can adsorb up to two adatoms while iridium clusters ($>0.6$ nm) adsorb a single adatom per exposed metal site.

## 1. INTRODUCTION

In recent years the selective chemisorption of gaseous molecules has been extensively used to estimate the degree of dispersion of supported Group VIII metal catalysts (*1*). Chemisorption methods are of special importance for highly dispersed catalysts since it is often difficult to establish the degree of dispersion by other procedures such as X-ray diffraction or electron microscopy measurements (*2*). The application of chemisorption measurements requires that adsorbate molecules form a surface monolayer and that adsorbate penetration into metal crystallites is negligible (*3, 4*). Interpretation of adsorbate uptakes also requires that a stoichiometric relationship exists between the number of molecules adsorbed and the number of exposed surface metal atoms (*3, 4*).

The selective chemisorption of hydrogen and carbon monoxide on alumina-supported platinum catalysts has been generally found to obey these criteria (*3–8*). The quantity of carbon monoxide adsorbed by a given platinum–alumina catalyst is approximately twice that of molecular hydrogen (*2*). The essentially two to one carbon monoxide to molecular hydrogen adsorption stoichiometry relationship results from the two adsorbates displaying different modes of interaction with the platinum surface. Upon adsorption molecular hydrogen dissociates into hydrogen atoms and it is assumed that one hydrogen atom is associated with each platinum surface atom (*4, 9*). The assumed hydrogen atom/surface platinum atom ratio (H/Pt) of unity has been confirmed by numerous BET and electron microscopy measurements (*3, 7, 8*). The adsorption of carbon monoxide is somewhat more complicated since this molecule can assume two different bonding configurations, namely, linear and bridge bonded surface species (*10*). In the linear configuration carbon monoxide is bonded via its carbon atom to a single platinum surface atom, while the bridged species, also bonded through carbon, is associated with two or more surface platinum atoms. The carbon monoxide/surface

0021-9517/80/090207-14\$02.00/0

platinum atom ratio (CO/Pt) is, therefore, dependent upon the relative quantities of linear and bridged entities. Comparative hydrogen and carbon monoxide chemisorption measurements on platinum catalysts suggest that the linear species predominants since H/Pt and CO/Pt ratios are found to be nearly equivalent (*7, 11*). Numerous infrared studies of carbon monoxide adsorbed on supported platinum catalysts also suggest the predominance of the linear bonded configuration (*12*). Thus, a large body of information exists which indicates that H/Pt and CO/Pt ratios are essentially equivalent to the fraction of exposed platinum atoms (*2*).

In contrast to supported platinum catalysts, the characterization of supported iridium catalysts by chemisorption measurements has received little attention (*12–17*). Reported studies do not reveal consistent values for the stoichiometries of hydrogen and carbon monoxide uptakes on supported iridium particles. The purpose of this paper is to describe in detail the hydrogen and carbon monoxide chemisorption properties of iridium–alumina catalysts. The present studies have shown iridium–alumina catalysts to exhibit much higher H/Ir and CO/Ir values than those typically displayed by platinum–alumina catalysts. A highly dispersed, 0.3 wt% iridium catalyst was, for example, found to exhibit limiting H/Ir and CO/Ir ratios approaching two. X-ray diffraction, transmission electron microscopy, and infrared measurements have been utilized to rationalize the high hydrogen and carbon monoxide uptakes displayed by iridium–alumina catalysts.

## 2. EXPERIMENTAL METHODS

### *Preparation of Iridium–Alumina Catalysts*

$\eta$-$Al_2O_3$ was prepared by calcining beta alumina trihydrate at 873 K in air for 16 hr. The $\eta$-$Al_2O_3$ employed in these studies had a BET surface area of 154 $m^2/g$. Supported iridium catalysts were prepared by incipient wetness impregnation of $\eta$-$Al_2O_3$ with an aqueous solution of chloroiridic acid. The impregnates were dried in air for 16 hr at 393 K and then mildly calcined under dry air at 540 K for an additional 4.0 hr. Iridium loadings for the four catalysts used in this study were determined to be 0.302, 1.04, 2.08, and 4.00 wt%, respectively (*18*).

### *Catalyst Agglomeration Treatment*

Oxidative calcinations of iridium–alumina catalysts were performed at 760 Torr total pressure by one of the following procedures: (a) calcining under dry air in a muffle furnace, (b) calcining under dry air or 20% $O_2$/He flowing at 500 $cm^3$/min in a quartz tube furnace, or (c) calcining under dry air (200–500 $cm^3$/min) in a quartz gas adsorption cell. Prior to oxidative calcination the catalysts were reduced under hydrogen (500 $cm^3$/min) for 2 hr at the corresponding calcination temperature. Preliminary studies established the extent of oxidative agglomeration to be reproducible if the catalysts were prereduced. Reduction temperatures of 673 to 873 K were found to have negligible effect on the dispersion of iridium–alumina catalysts.

### *Chemisorption Measurements*

Hydrogen and carbon monoxide chemisorption studies were performed with a conventional glass vacuum system (*12*). Ultimate dynamic vacua of about $10^{-7}$ Torr were obtainable. Pressure measurements during chemisorption studies were made with a Texas Instruments Precision Pressure gauge. Samples of 1 to 4 g, sieved to 20–40 mesh size, were placed in flow-through cells made of Vycor. All samples were reduced at 773 K under hydrogen (500 $cm^3$/min) *in situ* for 2 hr. The reduced samples were cooled to 723 K under hydrogen and evacuated at this temperature for 0.5 hr. The sample was then cooled under dynamic vacuum to room temperature (298 K). Longer reduction and evacuation times did not affect the subsequent chemisorption results.

Hydrogen and carbon monoxide uptakes

were determined at 298 ± 2 K on the reduced and evacuated samples. Typically, 0.5 hr was allowed for each uptake point. H(total)/Ir ratios were calculated by assuming that hydrogen uptakes at zero pressure correspond to saturation coverage of the metal. Total hydrogen uptake was determined by extrapolation of the high-pressure linear portion of the isotherm as described by Benson and Boudart and Wilson and Hall (*19*, *8*). Occasionally a second isotherm was measured after evacuating ($10^{-5}$ Torr) the sample following the initial isotherm at 298 K for 0.17 hr. The second isotherm provided a measure of the reversibly bound hydrogen at 298 K. The difference between these two isotherms gave the amount of hydrogen irreversibly (strongly) adsorbed at room temperature. CO/Ir ratios were calculated by determining the carbon monoxide uptakes on the reduced and evacuated samples and assuming that this represented the sum of carbon monoxide weakly bound to the support and strongly bound to the metal. The sample was then evacuated ($10^{-5}$ Torr) for 0.17 hr at room temperature and a second carbon monoxide isotherm measured. Since the second isotherm measured only the carbon monoxide weakly adsorbed on the support, subtraction of the two isotherms gave the quantity of strongly bound carbon monoxide which was associated with the metal. In accordance with previous studies, the amount of strongly bound carbon monoxide at 100 Torr was chosen as saturation coverage of the metal (*20*).

Hydrogen chemisorption measurements were also employed to ascertain the effects evacuation temperature and evacuation time had upon the coverage of hydrogen on iridium–alumina catalysts. Such measurements were performed sequentially as follows: An initial isotherm was determined on a reduced and evacuated sample at 298 K. The sample was evacuated ($10^{-5}$ Torr) at 298 K for 0.17 hr and a second isotherm was obtained. Subtraction of the two isotherms gave the amount of hydrogen irreversibly bound to the iridium surface at 298 K. A third isotherm was then determined at room temperature after evacuating ($10^{-5}$ Torr) the sample at 323 K for 0.17 hr. Subtraction of the third isotherm from the initial isotherm gave the quantity of irreversibly bound hydrogen held by iridium at 323 K. Additional isotherms were obtained after 0.17 hr evacuations ($10^{-5}$ Torr) at succeedingly higher temperatures up to a maximum of 623 K. In a similar fashion a series of room temperature isotherms were measured to determine the affect evacuation time (at 423 K) had on the hydrogen coverage of iridium–alumina catalysts.

BET surface areas were determined with argon at liquid nitrogen temperature (*21*). A value of 0.146 nm$^2$ was used for the area of an argon atom and a value of 210 Torr was used for $P_0$.

Hydrogen of 99.95% purity was passed through a Deoxo unit (Engelhard Industries, Inc.), a 5A molecular sieve drying trap, an Oxy-trap (Alltech Associates, Arlington Heights, Illinois) to remove last traces of oxygen and finally through a liquid nitrogen trap before being admitted to the catalyst for reductions or chemisorption measurements. Carbon monoxide of 99.99% purity was passed through a Dry Ice–isopropanol trap before exposure to the sample. Argon of 99.9995% purity was used after passage through an Oxy-trap.

### *X-Ray Diffraction Measurements*

A Philips Electronics X-ray diffractometer (XRG-3000) with nickel filtered Cu$K\alpha$ radiation was used for X-ray diffraction studies. Metal and metal-oxide crystallite sizes were calculated from line broadening data, as described elsewhere (*22*). Relative metal sintering rates were calculated using the 400 diffraction line of $\eta$- $Al_2O_3$ as an internal standard.

### *Transmission Electron Microscopy Measurements*

High-resolution transmission electron microscopy (TEM) investigations were performed on a Philips EM300 instrument with a line to line resolution better than 0.25 nm. The microscope and its calibration have been described by Prestridge and Yates (*23*). Transmission specimens were prepared from real catalyst samples by grinding and ultrasonically dispersing the powdered material in butyl alcohol (*24*). A drop of this suspension was then introduced onto a holey carbon film mounted on a conventional microscope grid (*25*). Specimens were dried and then examined in the TEM. With this arrangement it was possible to find sections of the catalyst which were extremely thin (<100 nm) and protruding from the carbon substrate. A number of electron micrographs were taken of these particular areas for each catalyst sample.

### *Infrared Measurements*

Infrared measurements were made with a Perkin-Elmer 621 spectrophotometer. The sample cell was of similar design to that described by Dent and Kokes (*26*). Catalysts were ground in an agate mortar to a fine powder and then a 90-mg sample was compressed under 103 MPa into a self-supporting 3.0-cm$^2$ wafer. The wafer was reduced under flowing hydrogen (200 cm$^3$/min) in the cell at 723 K for 1 hr and then evacuated ($10^{-5}$ Torr) at the reduction temperature for 0.5 hr prior to cooling to 298 K for experimental measurements.

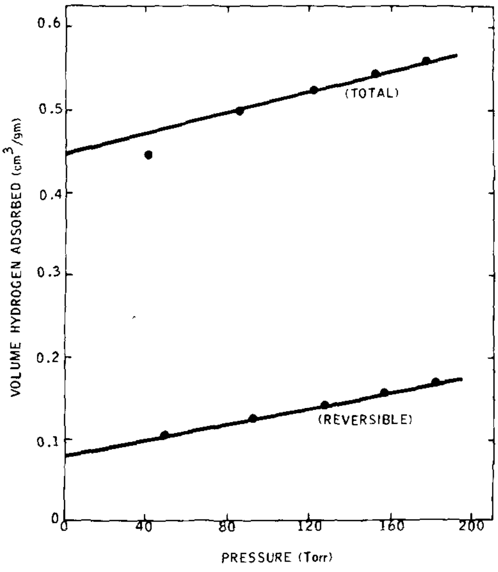

FIG. 1. Hydrogen adsorption isotherms at room temperature on a 0.3% iridium–alumina catalyst: total, initial $H_2$ isotherm; reversible, $H_2$ isotherm after evacuating sample following the initial isotherm for 0.17 hr at room temperature.

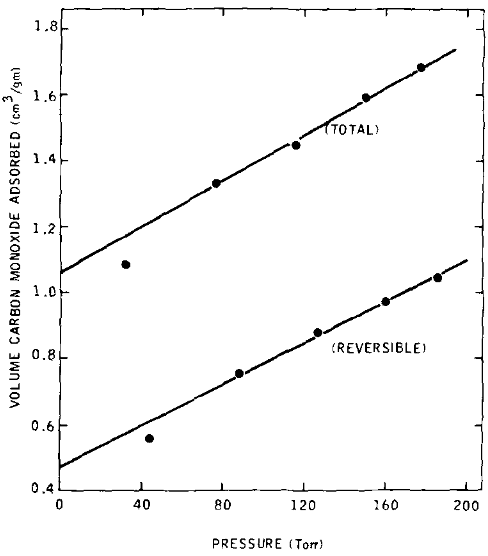

FIG. 2. Carbon monoxide adsorption isotherms at room temperature on a 0.3% iridium–alumina catalyst: total, initial CO isotherm; reversible, CO isotherm after evacuating sample following the initial isotherm for 0.17 hr at room temperature.

## 3. RESULTS

### *Chemisorption Measurements*

Typical room temperature hydrogen and carbon monoxide isotherms for a 0.3 wt% iridium–alumina catalyst are shown in Figs. 1 and 2, respectively. The quantity of the two gases adsorbed per gram of catalyst is expressed in terms of a gas volume corrected to standard conditions, i.e., 273 K and 760 Torr. From the zero pressure intercept of the total hydrogen uptake curve an H(total)/Ir ratio of 2.56 was calculated. The net irreversible hydrogen uptake at *zero* pressure was obtained by subtracting the reversible contribution from the initial uptake. Using this value, the H(irrev)/Ir ratio

TABLE 1

Comparison of Hydrogen and Carbon Monoxide Chemisorption on Iridium–Alumina Catalysts[a]

| Ir (wt%) | Adsorbate uptakes (μmole/g) | | | | Adsorbate/iridium ratios | | |
|---|---|---|---|---|---|---|---|
| | Total[b] | | Irreversible[c] | | H/Ir | | CO/Ir |
| | $H_2$ | CO | $H_2$ | CO | Total | Irreversible | Irreversible |
| 0.3 | 20.1 | 62.9 | 16.5 | 27.9 | 2.56 | 2.10 | 1.78 |
| 1.0 | 53.3 | 119.5 | 42.4 | 76.2 | 1.96 | 1.56 | 1.48 |
| 2.0 | 84.8 | 151.7 | 68.7 | 104.4 | 1.56 | 1.27 | 0.96 |
| 4.0 | 146.3 | 222.5 | 118.7 | 176.2 | 1.40 | 1.14 | 0.84 |

[a] Prior to reduction and chemisorption measurements the catalysts were calcined under 20% $O_2$/He (500 $cm^3$/min) at 543 K for 4.0 hr.

[b] Uptakes of $H_2$ and CO determined at 0 and 100 Torr, respectively.

[c] Quantity of $H_2$ and CO retained at 0 and 100 Torr, respectively, following a 0.17 hr evacuation ($10^{-5}$ Torr) at 298 ± 2 K.

was calculated to be 2.10. The quantity of carbon monoxide irreversibly bound to iridium at 298 K was obtained by subtracting the reversible fraction from the total uptake. The difference between the total and reversible adsorption curves at 100 Torr pressure was chosen to represent saturation coverage. From this value, the CO(irrev)/Ir ratio was calculated to be 1.78. It should be noted that a CO(irrev)/Ir ratio of 1.71 is obtained when the difference between the total and reversible uptake curves at zero pressure is used. Thus the usage of the difference between the total and reversible carbon monoxide adsorption curves at 100 Torr is arbitrary since the difference between the two curves is essentially pressure independent.

The chemisorption properties of a series of 0.3 to 4.0 wt% iridium–alumina catalysts were determined in a similar manner. The results of these studies are presented in Table 1. The volumetric uptakes of hydrogen and carbon monoxide have been converted to micromoles of adsorbates per gram of catalyst. The effect of iridium concentration on the reversible quantities of hydrogen and carbon monoxide at 298 K is shown in Fig. 3. The reversibly bound hydrogen curve extrapolates through the origin. This indicates that a negligible amount of hydrogen is physically adsorbed on the alumina support at room temperature. The quantity of carbon monoxide reversibly bound at room temperature, however, is not linearly dependent upon iridium concentration. This behavior suggests that a major fraction of the reversibly bound carbon monoxide is associated with the alumina support.

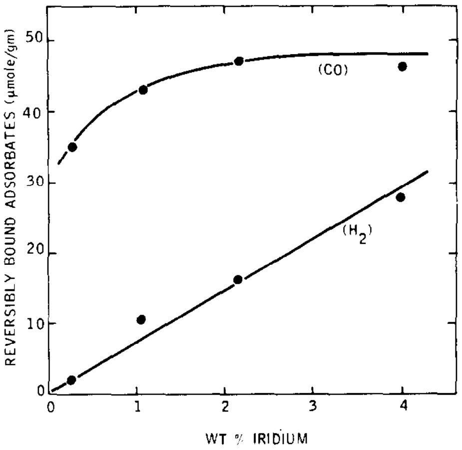

FIG. 3. The effect of iridium concentration on the reversible quantities of hydrogen and carbon monoxide bound by iridium–alumina catalysts at room temperature.

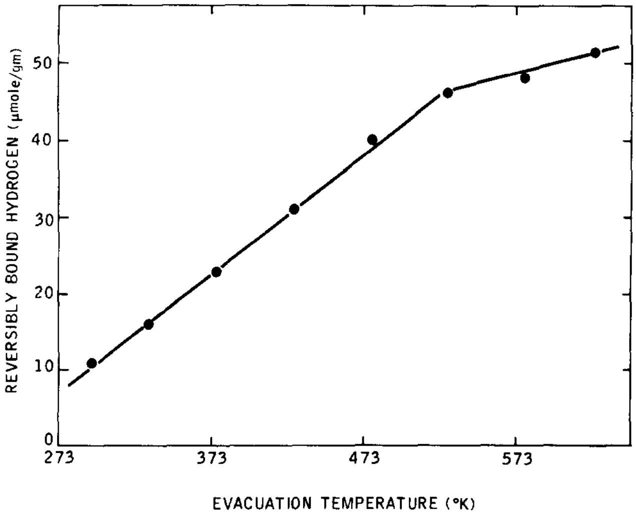

FIG. 4. The effect of evacuation temperature on the quantity of hydrogen removed from a 1% iridium-alumina catalyst. Initial uptake, 53.3 μmole hydrogen/g of catalyst.

The effect of evacuation temperature on the quantity of hydrogen removed from a fresh 1 wt% iridium-alumina catalyst is summarized in Fig. 4. The curve was obtained as follows: The initial room temperature uptake on a reduced and degassed sample was found to be 53.3 μmole of hydrogen per g of catalyst. The catalyst was then evacuated ($10^{-5}$ Torr) at 298 K for 0.17 hr and a second isotherm was measured. Upon readsorption an uptake corresponding to 10.9 μmole of hydrogen per g of catalyst was obtained. This value indicates that 20% (10.9/53.3) of the initial quantity of hydrogen can be removed from the iridium surface by evacuation at room temperature. Room temperature isotherms were subsequently measured on the same sample after evacuating for 0.17 hr at sequentially higher degassing temperatures. Temperatures in excess of 623 K were required to remove hydrogen completely from the iridium surface. The effect of time on the quantity of hydrogen desorbed from the 1% iridium catalyst at 423 K was also investigated. Over a 0.03 to 1.0 hr range of evacuation times the fraction of the initial hydrogen uptake (53.3 μmole/g) desorbed increased from 53 to 66%. Following a standard 0.17 hr evacuation, 60% of the initial room temperature uptake was desorbable. Thus increasing the evacuation time from 0.17 to 1.0 hr resulted in only a 6% increase in the quantity of hydrogen removed at 423 K. These results indicate that the ultimate quantity of hydrogen desorbed is primarily controlled by the degassing temperature and not by the time of evacuation.

The chemisorption properties of a series of partially agglomerated 1% iridium-alumina catalysts are summarized in Table 2. The oxidative agglomeration of iridium occurs readily at temperatures above 673 K (*27*). X-Ray diffraction measurements have shown that agglomeration takes place by the growth of $IrO_2$ crystallites. Prior to chemisorption measurements the alumina-supported $IrO_2$ agglomerates were reduced at 773 K under hydrogen. TGA studies have established that reduction to iridium metal readily occurs at temperatures near 450 K. The loss in iridium surface area is clearly indicated by the successive decreases in the H(total)/Ir and CO(irrev)/Ir ratios with calcination severity. Dispersions of the partially agglomerated catalysts have been normalized ($D/D_0$ values) with

TABLE 2

Comparison of Hydrogen and Carbon Monoxide Chemisorption on Agglomerated 1% Iridium–Alumina Catalysts[a]

| Sample number | Calcination treatment[b] | | Adsorbate/Ir ratios | | $D/D_0$[e] | |
|---|---|---|---|---|---|---|
| | °K | hr | $\frac{\text{H(total)}^c}{\text{Ir}}$ | $\frac{\text{CO(irrev)}^d}{\text{Ir}}$ | $H_2$ | CO |
| 1 | 543 | 4.0 | 1.96 | 1.48 | 1.00 | 1.00 |
| 2 | 723 | 0.25 | 1.57 | 1.12 | 0.80 | 0.76 |
| 3 | 723 | 0.50 | 1.43 | 1.06 | 0.73 | 0.72 |
| 4 | 748 | 0.50 | 0.98 | 0.67 | 0.50 | 0.45 |
| 5 | 773 | 0.25 | 0.79 | 0.56 | 0.40 | 0.38 |
| 6 | 773 | 0.50 | 0.66 | 0.44 | 0.34 | 0.30 |
| 7 | 773 | 1.0 | 0.51 | 0.38 | 0.26 | 0.26 |
| 8 | 773 | 2.5 | 0.36 | 0.24 | 0.18 | 0.16 |
| 9 | 773 | 4.0 | 0.28 | 0.21 | 0.14 | 0.14 |
| 10 | 873 | 8.0 | 0.13 | 0.10 | 0.07 | 0.07 |

[a] Prior to calcination, samples 2–10 were reduced under hydrogen (500 $cm^3$/min) at the corresponding calcination temperature for 2 hr.

[b] 20% $O_2$/He (500 $cm^3$/min).

[c] Total $H_2$ uptake at 0 Torr.

[d] Quantity of CO retained at 100 Torr following a 0.17 hr evacuation ($10^{-5}$ Torr) at 298 ± 2 K.

[e] Normalized dispersions.

respect to the H(total)/Ir and CO(irrev)/Ir ratios of the fresh catalyst (catalyst 1). The normalized dispersions for the two adsorbates were essentially identical over the wide range of dispersions investigated.

### *Transmission Electron Microscopy Measurements*

High-resolution transmission electron microscopy (TEM) examinations of a number of highly dispersed and partially agglomerated iridium–alumina catalysts were performed. The results of TEM measurements on a series of 1% iridium catalysts of varying dispersion are presented in Table 3. No iridium crystallites were detected upon repeated TEM examination of the fresh (sample 1) catalyst. Since 0.6-nm crystallites were easily observed in partially agglomerated samples (e.g., catalyst 4) it is reasonable to assume that the fresh catalyst contains crystallites less than 0.6 nm in diameter. Number average iridium crystallite sizes of the partially agglomerated catalysts were obtained from examination of at least six micrographs for each sample. The agglomerated catalysts clearly exhibit bimodal distributions of iridium crystallite sizes. As the degree of agglomeration was increased, the separation between the smallest and largest crystallites also increased. The majority of the crystallites in the more severely agglomerated samples were in the range 1.0 to 3.0 nm. Crystallites less than 5.0 nm in diameter were generally observed to be electron-transparent. This indicates that crystallites within this size range are extremely thin. At diameters above 5.0 nm the crystallites were noticeably more dense (electron-opaque) and are probably thicker.

### *Infrared Measurements*

The infrared spectra of carbon monoxide adsorbed on three 1% iridium–alumina catalysts of varying dispersion are shown in Fig. 5. Prior to recording the spectra each sample was dosed with 7 Torr carbon monoxide and then evacuated at room temperature. These spectra thus represent carbon monoxide irreversibly adsorbed on the iridium surface. The spectra under maximum (saturation) carbon monoxide coverage are clearly dependent upon iridium dispersion. The fresh, highly dispersed catalyst (CO/Ir

TABLE 3

Comparison of Chemisorption and TEM Measurements on Agglomerated 1% Iridium–Alumina Catalysts

| Sample number[a] | Crystallite size (nm) | | | | |
|---|---|---|---|---|---|
| | TEM | | | Chemisorption[b] | |
| | Minimum | Maximum | Average | $H_2$ | CO |
| 1 | <0.6 | <0.6 | <0.6 | <1.0 | <1.0 |
| 2 | <0.6 | <0.6 | <0.6 | <1.0 | <1.0 |
| 4 | 0.6 | 1.6 | 0.81 | 1.1 | 1.6 |
| 7 | 0.8 | 8.8 | 2.9 | 2.2 | 2.9 |
| 10 | 1.1 | 27.2 | 12.7 | 8.6 | 11 |

[a] Consult Table 2 for sample treatments.

[b] Spherical crystallite geometry assumed.

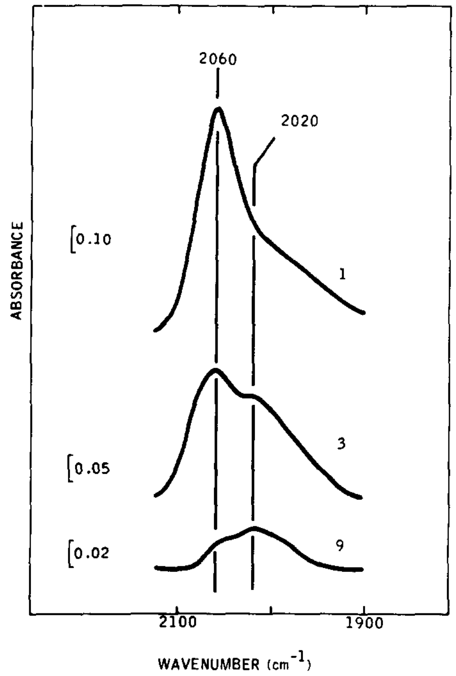

FIG. 5. The infrared spectra of carbon monoxide adsorbed on three 1% iridium–alumina catalysts of varying dispersion. Samples 1, 3, and 9 exhibited CO(irrev)/Ir ratios of 1.48, 1.06, and 0.21, respectively. Consult Table 2 for sample treatments.

= 1.48) exhibited a strong carbon monoxide stretching frequency centered at 2060 cm$^{-1}$ and a weaker shoulder at 2020 cm$^{-1}$. At lower iridium dispersion levels (CO/Ir = 1.06 and 0.21, respectively) the relative intensity of the 2020 cm$^{-1}$ band increased progressively at the expense of the 2060 cm$^{-1}$ band.

The stretching frequency of carbon monoxide adsorbed upon the fresh 1% iridium catalyst (CO/Ir = 1.48) was also observed to be dependent upon the extent of carbon monoxide coverage (see Fig. 6). At less than monolayer coverage (CO/Ir = 0.3), a sample annealed at 373 K for 0.5 hr exhibited a carbon monoxide stretching band centered at 2025 cm$^{-1}$. Under maximum coverage (CO/Ir = 1.48), the sample displayed, as noted earlier, a strong band at 2060 cm$^{-1}$ and a weak shoulder in the 2020–2025 cm$^{-1}$ region. Evacuating this sample at 523 K for 0.5 hr lowered the CO/Ir ratio from its maximum value of 1.48 to a value near 1.0. Concomitant with the change from maximum to monolayer coverage was the complete loss of the 2060 cm$^{-1}$ band. The band at 2025 cm$^{-1}$, however, was retained upon evacuation.

## 4. DISCUSSION

### *Chemisorption and TEM Studies on Highly Dispersed Iridium–Alumina Catalysts*

The iridium–alumina catalysts employed in this study were prepared by the incipient wetness impregnation of $\eta$-$Al_2O_3$ with dilute, aqueous chloroiridic acid solutions. Maximum iridium surface areas were obtained by calcining the catalysts at 520–540 K under air, prior to reduction with hydrogen. The mild air calcination treatments are thought to anchor iridium onto special acceptor sites on the alumina surface. Iridium surface areas are stable under hydrogen as no decreases in dispersion were detected

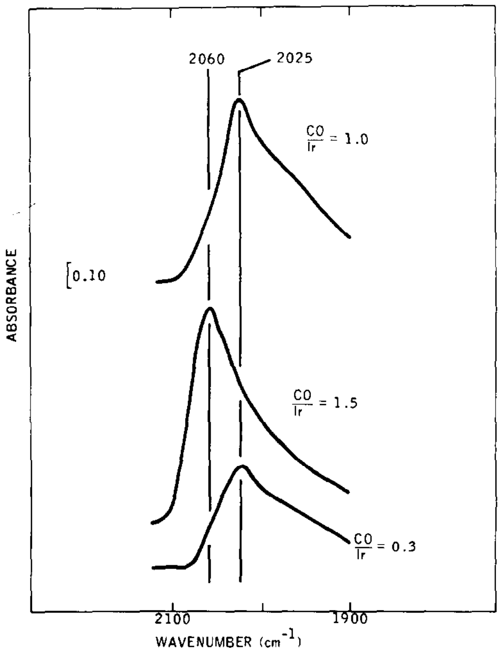

FIG. 6. The effect of surface coverage on the infrared spectrum of carbon monoxide adsorbed on a highly dispersed 1% iridium–alumina catalyst (sample 1 in Table 2).

over a 673 to 873 K range of reduction temperatures. Representative hydrogen and carbon monoxide isotherms for a 0.3 wt% iridium–alumina catalyst are shown in Figs. 1 and 2, respectively. Equilibrium uptakes of hydrogen and carbon monoxide were rapid. Approximately 90 to 95% of the total adsorption is instantaneous. The net irreversible hydrogen and carbon monoxide adsorption was obtained by subtracting the reversible fraction from the total uptakes at zero and 100 Torr pressure, respectively. Using these irreversible uptake values H(irrev)/Ir and CO(irrev)/Ir ratios of 2.10 and 1.78, respectively, were calculated. These ratios represent the average numbers of hydrogen atoms and carbon monoxide molecules that are strongly adsorbed per exposed iridium atom at room temperature. The use of adsorbate/iridium ratios to characterize these catalysts instead of average crystallite sizes or percentage dispersion is preferred since assumptions involving surface coverage and adsorption stoichiometries are not required (*4*). By way of comparison, a 0.3 wt% platinum–alumina catalyst was found to exhibit H(irrev)/Pt and CO(irrev)/Pt ratios of 0.69 and 0.75, respectively. Thus in contrast to platinum, iridium has the ability to irreversibly bind up to two adsorbate atoms or molecules per exposed metal atom. A minimum of six TEM examinations of the fresh 0.3% iridium catalyst did not indicate the presence of any metal crystallites. Small, 0.6-nm-diameter crystallites were, however, observed by TEM in catalysts subjected to oxidative agglomeration treatments. It is, therefore, reasonable to assume then that a fresh 0.3 wt% iridium catalyst contains metal crystallites less than 0.6 nm in diameter. A 0.6-nm crystallite constructed by f.c.c. packing could accommodate a maximum of six iridium atoms (*28*). An incomplete f.c.c. crystallite, down to a minimum of two atoms, could in principle also be detected by TEM as 0.6-nm clusters. The absence of detectable metal particles in the fresh 0.3 wt% iridium catalyst indicates that iridium is in the form of small clusters which contain fewer than six atoms and may in fact approach single atom dispersion.

As the concentration of iridium was increased from 0.3 to 4 wt% the adsorbate/iridium ratios were observed to decrease by a factor of approximately two (see Table 1). The H(irrev)/Ir ratios, however, remained above unity throughout this concentration range. The systematic lowering of the adsorbate/iridium ratios with increasing iridium concentration may reflect the expected decrease in dispersion at higher metal loading levels (*7*, *20*). For a given catalyst the H(irrev)/Ir ratios are 1.1 to 1.4 times larger than the corresponding CO(irrev)/Ir ratios. The difference between these ratios increases in the direction of higher iridium concentration. This indicates that the fraction of carbon monoxide molecules adsorbed in bridging configurations is higher in the more concentrated catalysts. Similar metal concentration effects have been reported for platinum–alumina catalysts (*4*).

The quantity of reversibly bound hydrogen at room temperature was found to be linearly dependent upon iridium concentration (see Fig. 3). Upon extrapolation, the reversibly bound hydrogen curve passes through the origin. Thus the major fraction of the weakly bound hydrogen is associated with the iridium component and not physically adsorbed on the alumina support. This behavior indicates that hydrogen spillover (*29*) does not have to be envoked to account for the high H(total)/Ir ratios displayed by 0.3 to 4 wt% iridium–alumina catalysts. The amount of weakly associated carbon monoxide was, however, observed to be much less dependent upon the concentration of iridium. The reversibly bound carbon monoxide curve indicates that most of the weakly held carbon monoxide is physically adsorbed on the alumina support. Thus in contrast to hydrogen adsorption, it is imperative that a correction for the physically adsorbed carbon monoxide is made. This correction is especially important at lower iridium loading levels.

The possibility of hydrogen-spillover in a 1% iridium–alumina catalyst was further investigated by studying the effect temperature had upon the quantity of adsorbed hydrogen removed at $10^{-5}$ Torr (see Fig. 4). The amounts of hydrogen desorbed were found to increase linearly from 298 K up to about 523 K. At 523 K approximately 85% of the initial room temperature hydrogen uptake was removed by a 0.17 hr evacuation. Temperatures in excess of 623 K were required to remove hydrogen completely from the iridium surface. The linear, incremental desorption of hydrogen with increasing temperature indicates that the H–Ir chemisorption bond strength increases smoothly with decreasing surface coverage. Analogous behavior has been reported for platinum–alumina catalysts (*30, 31*). The shape of the desorption curve suggests the absence of hydrogen spillover since it is reasonable to assume that a break in the curve would have occurred between 373 and 423 K where the H/Ir ratio is near one if desorption of spilled-over hydrogen were occurring. The demonstration of a 1.48 CO(irrev)/Ir ratio by the 1% iridium catalyst lends credence to the suggestion that hydrogen spillover is not responsible for the high H(irrev)/Ir ratio of 1.56 exhibited by this catalyst.

### *Chemisorption and TEM Studies on Partially Agglomerated Iridium–Alumina Catalysts*

The chemisorption properties of a 1% iridium–alumina catalyst subjected to a series of oxidative calcination treatments are summarized in Table 2. Progressive agglomeration of iridium is reflected in decreasing H(total)/Ir and CO(irrev)/Ir ratios. The two adsorbate/iridium ratios were observed to be highly dependent upon calcination temperature. Comparison of the sample pairs 3 and 4 or 4 and 6 shows that a 25 K increase in calcination temperature lowers the hydrogen and carbon monoxide uptakes by approximately 35%. These results indicate that the adsorbate/iridium ratios are extremely sensitive to subtle changes in crystallite sizes. The apparent activation energy for the oxidative agglomeration of iridium is 16.5 kcal/mole, thus a 25 to 50 K increase in calcination temperature would not be expected to increase drastically the size of the iridium crystallites (*27*). For a given calcination treatment the H(total)/Ir ratio is 1.4 to 1.5 times larger than the corresponding CO(irrev)/Ir ratio. These differences, however, are eliminated when comparison is made on a normalized basis. The normalized chemisorption values ($D/D_0$) for a particular sample indicate comparable relative dispersion levels. Such agreement suggests that iridium crystallites of varying sizes affect the uptakes of hydrogen and carbon monoxide to the same degree. X-ray diffraction measurements on a number of agglomerated samples show the presence of iridium crystallites much larger than those calculated from chemisorption data. Sample 7, for example, displayed X-ray line widths indicative of 17-nm crystallites. Assuming a spherical crystallite geometry, hydrogen and carbon monoxide chemisorption uptakes indicate average iridium crystallite sizes of 2.2 and 2.9 nm, respectively, for this sample (*32*). The disparity between average crystallite sizes calculated from X-ray diffraction and chemisorption measurements demonstrates that agglomerated iridium–alumina catalysts contain a bimodal distribution of crystallite sizes.

The bimodal nature of agglomerated iridium–alumina catalysts was quantified by TEM measurements. Average crystallite sizes observed directly by TEM measurements for a series of partially agglomerated 1% iridium catalysts are presented in Table 3. No iridium crystallites were detected on the fresh catalyst (sample 1). Extremely small, 0.6-nm-diameter clusters were, however, detected in several oxygen calcined samples (note sample 4). As stated earlier a maximum of six iridium atoms could be accommodated in a cluster of this size. The absence, therefore, of detectable particles indicates that the fresh catalyst must be composed of single atoms or clusters with fewer than six atoms. As the calcination severity was increased (samples 7 and 10) the separation between the largest and smallest sized clusters became larger. Agreement was obtained between the largest crystallites seen in TEM examinations and those calculated from X-ray line broadening measurements. The greatest number of observable crystallites were in the range 1.0 to 3.0 nm in diameter. The preponderance of smaller crystallites yields number average crystallize sizes which are significantly smaller than the largest crystallites present in each sample. Crystallites less than 5.0 nm in diameter were observed to be electron-transparent and irregularly shaped. Similar crystallite morphology has been reported for iridium–silica catalysts (*33*). At diameters above 5.0 nm the crystallites remained irregularly shaped but became noticeably more dense (electron-opaque). The higher density noted in the larger crystallites indicates the possible transformation into energetically more favorable three-dimensional geometries.

The high adsorbate/iridium ratios exhibited by the fresh 1% iridium catalyst are in agreement with the high dispersion indicated by the absence of TEM detectable particles. The initial H(irrev)/Ir and CO(irrev)/Ir ratios of 1.56 and 1.48, respectively, indicate that multiple adsorbate bonding is occurring either on isolated atoms or coordinately unsaturated corner and edge atoms of small crystallites. It is well established that coordinately unsaturated atoms are in significant numbers only in small (<2-nm) metal crystallites. To illustrate this point, the percentage corner plus edge atoms in a f.c.c. packed crystallite of iridium would decrease from 93 to 10% upon a crystallite diameter increase of 1.0 to 3.0 nm (*28*). The rapidly decreasing number of corner and edge atoms with crystallite growth is accompanied by an increase in the fraction of face and bulk atoms. From steric considerations it is reasonable to assume that iridium atoms on a crystallite face can adsorb only one hydrogen atom or one carbon monoxide molecule (*24*). Based upon this model, the high adsorbate/iridium ratios exhibited by the fresh 1% iridium catalyst require that a major fraction of iridium is either monoatomically dispersed or is in the form of small clusters containing fewer than six atoms.

Sample 2 exhibited H(total)/Ir and CO(irrev)/Ir ratios of 1.57 and 1.12, respectively. The mild calcination experienced by sample 2 produced a 20–25% decrease in the uptakes of hydrogen and carbon monoxide, however, the catalyst was found to remain TEM amorphous. These results are extremely significant since they demonstrate that small changes in iridium cluster size below the limit of TEM detectability markedly affects the adsorbate/Ir ratios. The data suggest that TEM amorphous particles containing less than six atoms are formed during the early stages of agglomeration by the clustering of monoatomically dispersed iridium atoms. The chemisorption results further indicate that such clusters are incapable of binding two adsorbate atoms or molecules per exposed metal atom. These results may be rationalized if it is assumed that only isolated iridium atoms can accommodate two adsorbate atoms or molecules. The generation of small (<0.6 nm) clusters containing four or five atoms requires the formation of metal–metal bonds. Cluster formation may restrict adsorption to a single adatom per exposed metal atom since potential adsorption sites present on atomically dispersed iridium atoms are utilized in metal–metal bond formation. An alternate explanation might be that monoatomically dispersed iridium atoms are modified by a support interaction which facilitates the adsorption of two adatoms.

The average crystallite sizes calculated from chemisorption data and directly observed by TEM measurements for the more highly agglomerated catalysts (samples 4, 7 and 10) were found to be in fair agreement. The average crystallite sizes derived from chemisorption data were calculated assuming spherical particle geometries and a 1 : 1 adsorbate : surface metal atom stoichiometry (*20*). The agreement between crystallite sizes obtained by TEM and chemisorption approaches supports the suggestion that isolated iridium atoms are principally responsible for binding up to two adsorbate atoms or molecules per exposed metal atom. Justification for this line of reasoning is the following: Samples 4 and 7 have been shown by TEM to contain a sizable number of clusters 1.0 nm and less in diameter. The adsorption of two adatoms on coordinately unsaturated atoms present on clusters in this size range would have biased the average crystallite sizes calculated from chemisorption data toward smaller diameters. Since such a bias was not obtained it is reasonable to suggest that iridium clusters of the order of 1.0 nm in diameter exhibit a 1 : 1 adsorbate : exposed metal atom stoichiometry. The comparable average crystallite sizes obtained from chemisorption and TEM measurements also indicate that partially agglomerated iridium catalysts do not contain a significant number of monoatomically dispersed metal atoms since their presence would have also biased the chemisorption derived crystallite sizes to smaller values.

### *Infrared Studies of Highly Dispersed and Partially Agglomerated Iridium–Alumina Catalysts*

The infrared spectra of carbon monoxide adsorbed on three 1% iridium–alumina catalysts of varying dispersion (CO(irrev)/Ir = 0.21 to 1.48) are presented in Fig. 5. The three catalysts correspond to sample treatments 1, 3, and 9 outlined in Table 2. These spectra, recorded under conditions of maximum (irreversible) coverage of the iridium surface by carbon monoxide, are clearly dependent upon the level of iridium dispersion. The most highly dispersed sample (CO(irrev)/Ir = 1.48) exhibited a strong, relatively sharp carbon monoxide stretching frequency centered at 2060 $cm^{-1}$ and a weaker shoulder situated near 2020 $cm^{-1}$. The positions of these band maxima are in good agreement with the spectra reported for carbon monoxide adsorbed on silica- and alumina-supported iridium catalysts (*33–35*). Based upon the multiple carbon monoxide uptakes and the fact that the fresh catalyst is TEM amorphous, it is reasonable to assume that the 2060 $cm^{-1}$ band results from the simultaneous adsorption of two carbon monoxide molecules on isolated iridium atoms. The shoulder near 2020 $cm^{-1}$ likely results from the adsorption of one carbon monoxide molecule per iridium atom. Metal sites giving rise to the 2020 $cm^{-1}$ band may contain a small number (two to six) of iridium atoms which exhibit a lower carbon monoxide adsorption stoichiometry than isolated metal atoms. At lower dispersion levels CO(irrev)/Ir = 1.06 and 0.21, respectively, the relative intensity of the 2020 $cm^{-1}$ band progressively increases at the expense of the 2060 $cm^{-1}$ band. The growth of the 2020 $cm^{-1}$ band with decreasing dispersion is consistent with the adsorption of carbon monoxide on an increasing fraction of larger iridium crystallites. TEM and adsorption uptake data further indicate that larger iridium crystallites can accommodate a maximum of one carbon monoxide per exposed metal site. The presence of the 2060 $cm^{-1}$ band in agglomerated samples is consistent with the known bimodel distribution of iridium crystallite sizes (*27*). The shift in band maxima from 2060 to 2020 $cm^{-1}$ upon clusterification of iridium atoms indicates that back-bonding is lowest in the case of isolated atoms (*37*, *38*).

The stretching frequency of carbon monoxide adsorbed on the highly dispersed (CO/Ir = 1.48) sample was found to be dependent upon surface coverage (see Fig. 6). At less than monolayer coverage (CO/Ir = 0.3) a sample annealed at 373 K for 0.5 hr exhibited a carbon monoxide stretching frequency centered near 2025 $cm^{-1}$. The sample was annealed at 373 K to ensure distribution of carbon monoxide throughout the wafer. Under maximum coverage conditions (CO/Ir = 1.48) the band maxima shifted to 2060 $cm^{-1}$. Evacuating this sample at 523 K for 0.5 hr lowered the CO/Ir ratio from its maximum value of 1.48 to a value near 1.0. Concomitant with the change from maximum to monolayer coverage the carbon monoxide frequency is displaced from 2060 to 2025 $cm^{-1}$. These observations can be rationalized as follows: The 2060 $cm^{-1}$ band is associated with an isolated iridium atom which can accommodate the adsorption of two carbon monoxide molecules. Theoretically, dicarbonyl species such as $Ir(CO)_2$ possess local $C_{2v}$ symmetry and infrared bands corresponding to symmetric and antisymmetric fundamental modes are expected (*36*). The absence of detectable splitting in the 2060 $cm^{-1}$ band indicates that the symmetric and antisymmetric modes are weakly coupled. Weak coupling between these modes is possible if the carbon monoxide molecules are not equivalently bonded to the iridium atom. The fact that the 2060 $cm^{-1}$ band disappears upon evacuation at elevated temperatures indicates that one carbon monoxide molecule is more readily removed than the other. This observation supports a surface species such as Ir(CO)(CO) which contains nonequivalent carbon monoxide molecules (*33*). The basis for the nonequivalency is not known at this time. The band centered in the 2020–2025 $cm^{-1}$ region results from the adsorption of a single carbon monoxide molecule per iridium atom. The position of this lower frequency band is essentially insensitive to changes in surface coverage or crystallite size. The shift to higher frequencies upon adsorption of a second carbon monoxide molecule suggests that doubly occupied iridium sites have lower effective electron densities than singly occupied sites (*37, 38*). The infrared spectra of carbon monoxide adsorbed on iridium–alumina catalysts thus allow the qualitative differentiation between iridium sites which doubly and singly adsorb carbon monoxide molecules.

## 5. SUMMARY

Highly dispersed iridium–alumina catalysts, containing metal crystallites less than 0.6 nm in diameter, have been found to exhibit unusually high, irreversible uptakes of hydrogen and carbon monoxide. Catalysts containing 1% or less iridium displayed H/Ir and CO/Ir ratios which approached limiting values of two. The results of hydrogen desorption studies indicated that the high H/Ir ratios are not a consequence of hydrogen spillover onto the alumina support. TEM measurements in concert with chemisorption uptakes indicated that multiple adsorbate bonding occurs primarily on monoatomically dispersed iridium atoms and not on coordinately unsaturated corner and edge atoms of small (0.6–2 nm) crystallites. Average crystallite sizes calculated from chemisorption data and observed directly by TEM for partially agglomerated catalysts were found to be in good agreement. Agreement was best achieved when it was assumed that crystallites 0.6 nm in diameter and larger exhibit a 1 : 1 adsorbate : exposed metal atom stoichiometry. Finally, infrared spectra were found to differentiate iridium sites which doubly and singly adsorb carbon monoxide molecules.

## ACKNOWLEDGMENTS

The authors wish to thank Mr. J. J. Ziemiak and Mrs. L. W. Turaew for their valuable experimental assistance. The authors are especially indebted to professors M. Boudart and E. G. Derouane for their many helpful discussions.

## REFERENCES

1. Muller, J., *Rev. Pure Appl. Chem.* **19,** 151 (1969).
2. Sinfelt, J. H., *Ann. Rev. Mat. Sci.* **2,** 641 (1972).
3. Spenadel, L., and Boudart, M., *J. Chem. Phys.* **64,** 204 (1960).
4. Gruber, H. L., *J. Chem. Phys.* **66,** 48 (1962).

5. Dautzenberg, F. M., and Wolters, H. B. M., *J.Catal.* **51,** 26 (1978).
6. Adler, S. F., and Keavney, J. J., *J. Phys. Chem.* **64,** 208 (1960).
7. Renouprez, A., Hoang-Van, C., and Compagnon, P. A., *J. Catal.* **34,** 411 (1974).
8. Wilson, G. R., and Hall, W. K., *J. Catal.* **17,** 190 (1970).
9. Sinfelt, J. H., *Catal. Rev.* **3,** 175 (1969).
10. Eischens, R. P., and Pliskin, W. A., *Advan. Catal.* **10,** 1 (1958).
11. Yates, D. J. C., and Sinfelt, J. H., *J. Catal.* **14,** 182 (1969).
12. Sinfelt, J. H., and Yates, D. J. C., *J. Catal.* **8,** 82 (1967).
13. Brooks, C. S., *J. Colloid Interface Sci.* **34,** 419 (1970).
14. Moroz, E. M., Bogdanov, S. V., Buyanova, N. E., and Kovrizhina, O. V., *Kinet. Katal.* **19,** 1029 (1978).
15. Anderson, J. R., Elmes, P. S., Howe, R. F., and Mainwaring, D. E., *J. Catal.* **50,** 508 (1977).
16. Fiedorow, R. M., Chahar, B. S., and Wanke, S. E., *J. Catal.* **51,** 193 (1978).
17. Anderson, J. R., and Howe, R. F., *Nature (London)* **268,** 129 (1977).
18. Analyses were performed by the Analytical and Information Division, Exxon Research and Engineering Company, Linden, New Jersey.
19. Benson, J. E., and Boudart, M., *J. Catal.* **4,** 704 (1965).
20. Yates, D. J. C. and Sinfelt, J. H., *J. Catal.* **8,** 348 (1967).
21. Brunauer, S., Emmett, P. H., and Teller, E., *J. Amer. Chem. Soc.* **60,** 309 (1938).
22. Klug, H. P., and Alexander, L. E., *in* "X-ray Diffraction Procedures for Polycrystalline and Amorphous Materials," 2nd ed., p. 687. Wiley, New York, 1974.
23. Prestridge, E. B., and Yates, D. J. C., *Nature (London)* **234,** 345 (1971).
24. Yates, D. J. C., Murrell, L. L., and Prestridge, E. B., *J. Catal.* **57,** 41 (1979).
25. Bradley, D. E., *in* "Techniques for Electron Microscopy" (D. H. Kay, Ed.), 2nd ed., p. 71. Davis, Philadelphia, 1965.
26. Dent, A. L., and Kokes, R. J., *J. Amer. Chem. Soc.* **92,** 6709 (1970).
27. McVicker, G. B., Garten, R. L., and Baker, R. T. K., *J. Catal.* **54,** 129 (1978).
28. Von Hardeveld, R., and Hartog, F., *Surface Sci.* **15,** 189 (1969).
29. Boudart, M., Vannice, M. A., and Benson, J. E., *Z. Phys. Chem. (N.F.)* **64,** 171 (1969).
30. Cusumano, J. A., Dembinski, G. W., and Sinfelt, J. H., *J. Catal.* **5,** 471 (1966).
31. Kubokowa, Y., Takashima, S., and Toyama, O., *J. Phys. Chem.* **8,** 1244 (1964).
32. The average crystallite sizes were calculated from the relationship $D = 6 \times 10^4/Sb$ where $D$ is the diameter of the crystallite in Å, $S$ is the surface area in $m^2/g$, and $b$ is the density of iridium.
33. Guerra, C. R., and Schulman, J. H., *Surface Sci.* **7,** 229 (1967).
34. Howe, R. F., *J. Catal.* **50,** 196 (1977).
35. Lynds, L. *Spectrochim. Acta* **20,** 1369 (1964).
36. Herzberg, G., *in* "Molecular Spectra and Molecular Structure," Vol. II, p. 106. Van Nostrand, New York, 1964.
37. Orgel, L. E., *Inorg. Chem.* **1,** 25 (1962).
38. Primet, M., Basset, J. M., Mathieu, M. V., and Prettre, M., *J. Catal.* **29,** 213 (1973).